Discussion:

Measurement of the evolution of a plasma column by modulation of a high-energy proton beam

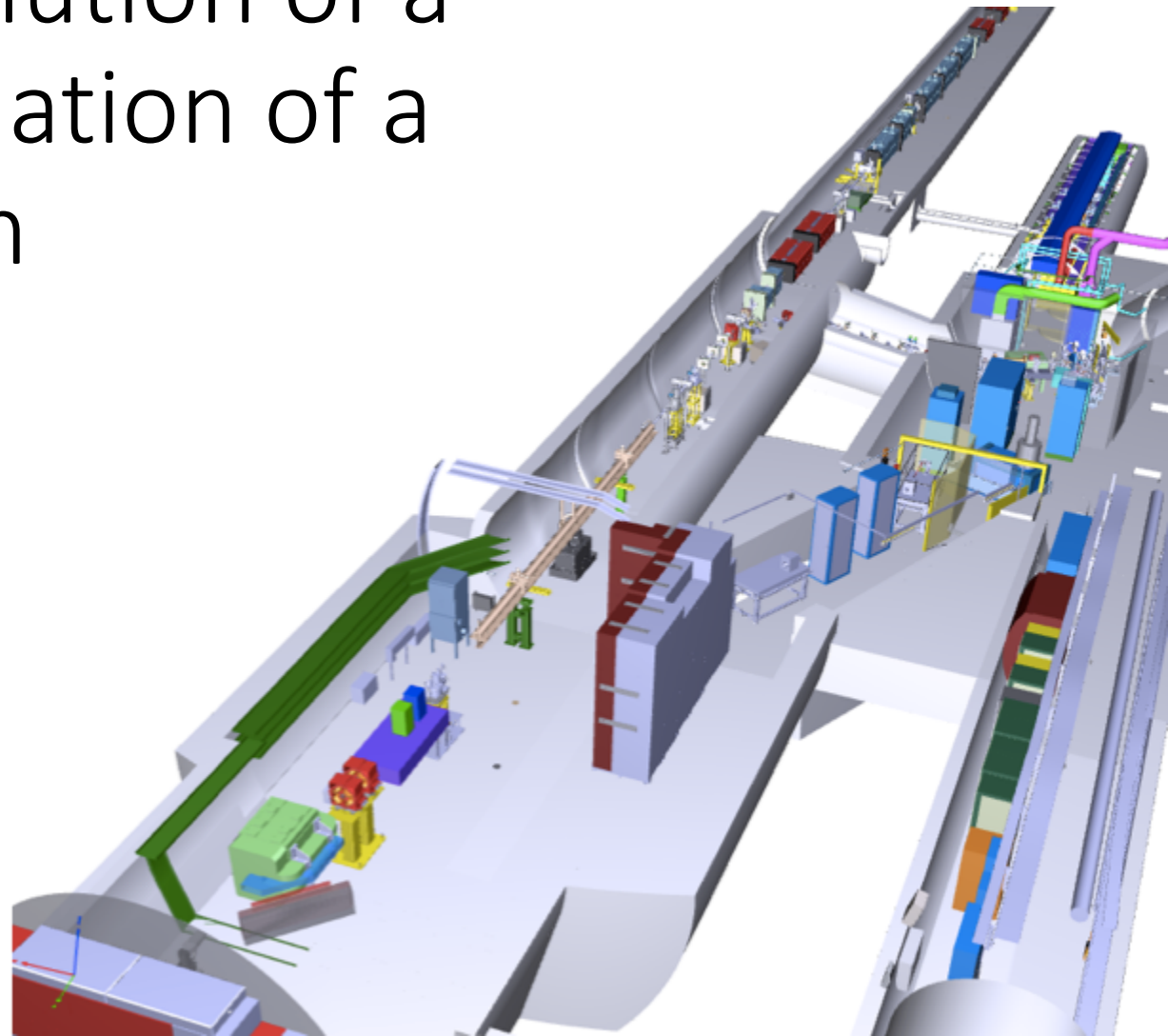

Spencer Gessner

11 June, 2019

I received valuable input and feedback from *many* people in the AWAKE collaboration in all stages of this process.

Thank you to everyone who contributed to the data taking, analysis, modeling, and checking the manuscript.

Outline

1. Measurement and Motivation
2. Data and Error Analysis
3. Model
4. Review of Figures
5. Updates to the Manuscript

Motivation for measurement

During AWAKE's first experimental runs in 2017, we varied the timing of the ionizing pulse with respect to the proton beam in order to study the stability of SSM. This led to several studies:

1. Stability of SSM. (F. Batsch)
2. Appearance of hosing instability. (M. Hüter).
3. Modulation growth rate. (A. Bachmann)

We also observed that even when the laser pulse is *very far ahead* of the proton beam, we still see modulation of the proton bunch. Motivation for this study:

- How long does the plasma last and how does it evolve?

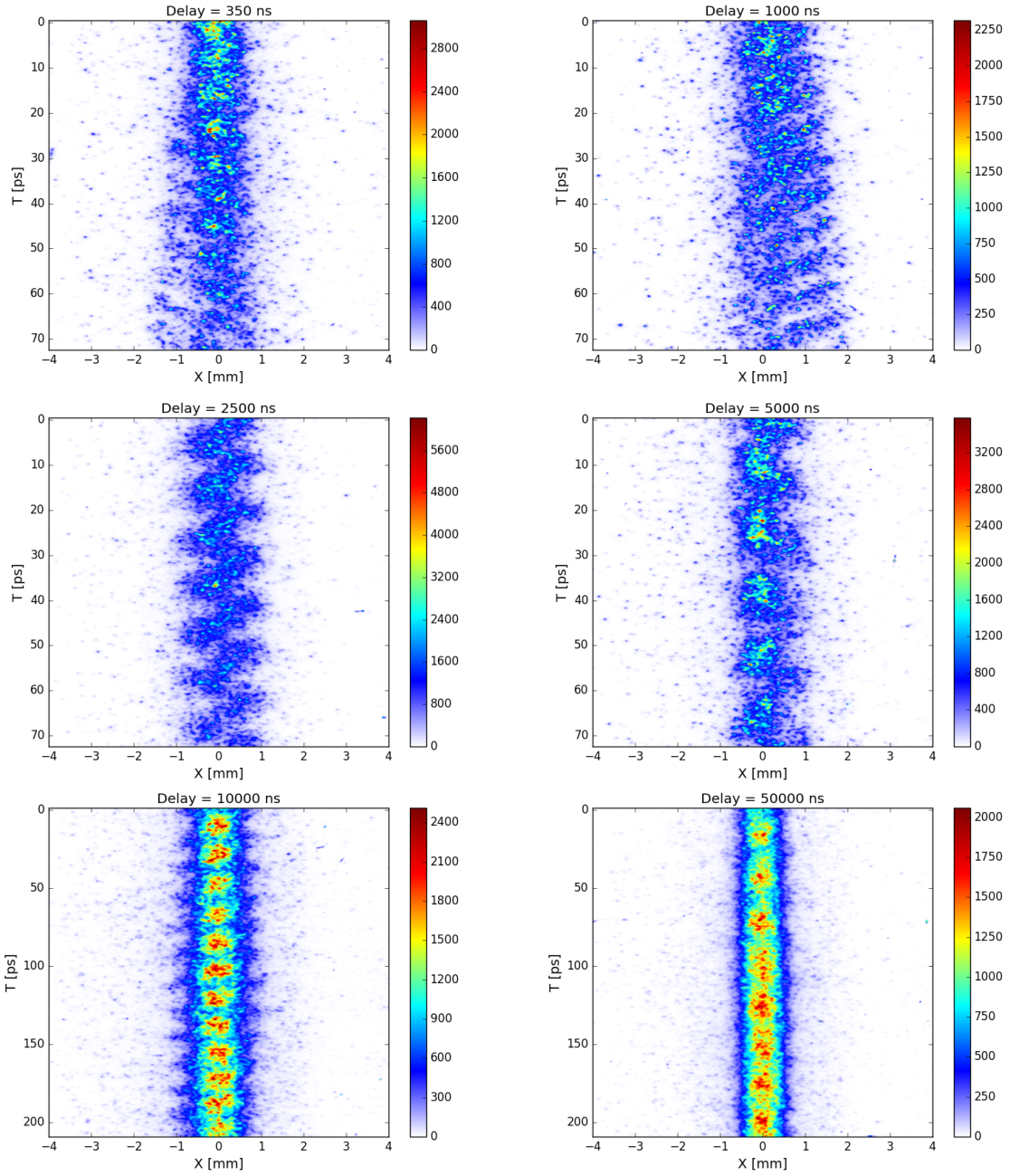

Overview of the Datasets

We performed long time delay scans on:

- 5 June, 2017
- 3 September, 2017
- **13 May, 2018**
- 25 September, 2018

We get the same qualitative result for each dataset, but the data from 13 May was acquired in the most rigorous, controlled way.

For the data acquired on 13 May, 2018, we scanned both the time delay and the laser pulse energy.

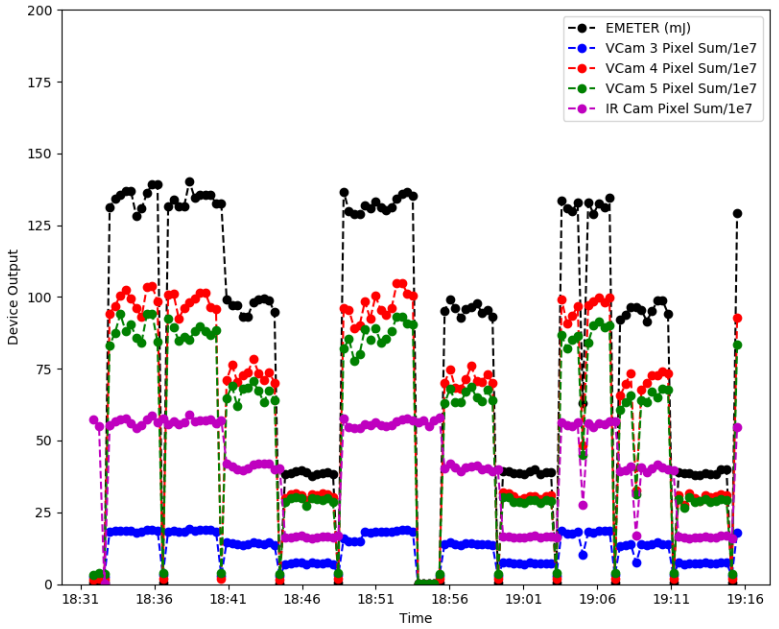

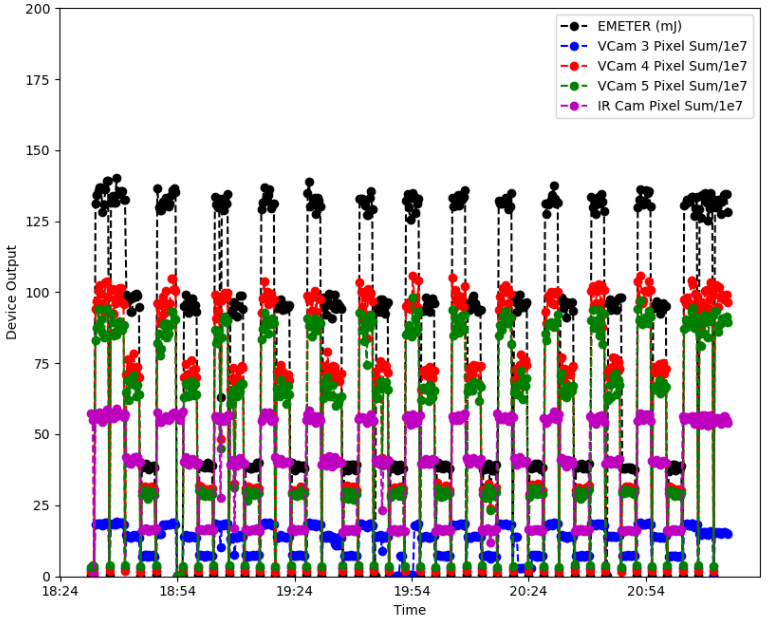

Outline

1. Measurement and Motivation
2. Data and Error Analysis
3. Model
4. Review of Figures
5. Updates to the Manuscript

Streak Camera Projection Analysis

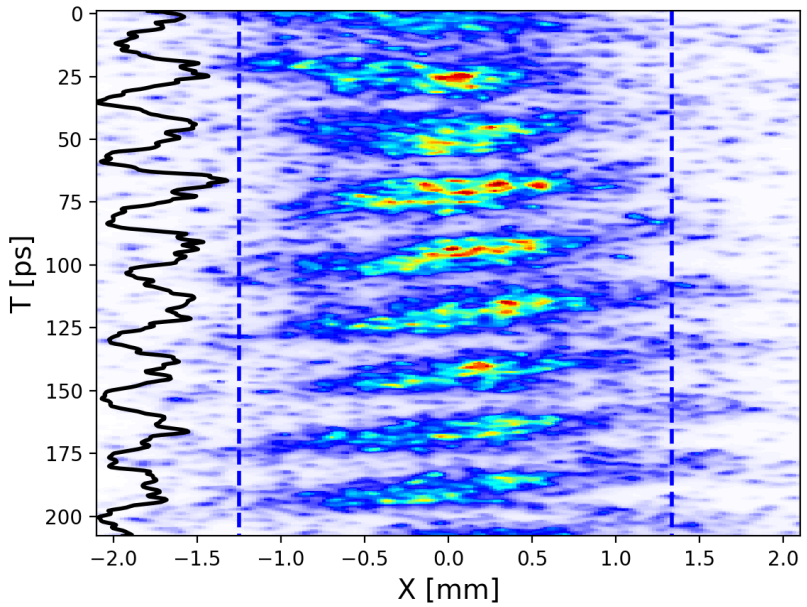

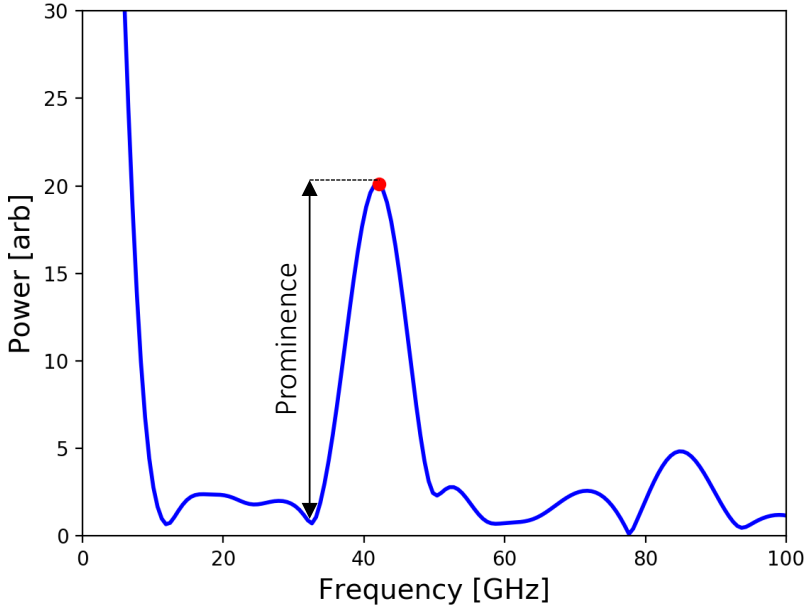

Starting from the streak camera image, we take a projection (black line), apply a Hann filter, and embed the projection in a zero-padded array. The procedure is similar to the one used in "Experimental Observation of Proton Bunch Modulation in a Plasma at Varying Plasma Densities" AWAKE Collab. *PRL* 054802 (2018).

The peak frequency is identified by "prominence": the height of the local maximum with respect to the nearest local minimum on the low frequency side of the spectrum. This definition is useful for discriminating against the large DC content of the spectrum.

Using this procedure, the resolution of the measurement is 1.2 GHz (2 GHz in the *PRL*).

Treating a single image as several measurements

Another way to analyze the streak camera image is to take the FFT of every column and find the peak frequency for each column.

The frequencies are entered into a histogram, with each entry weighted by prominence.

The peak frequency for the image is extracted from a gaussian fit to the histogram.

This is a sensible approach if each column is an independent measurement.

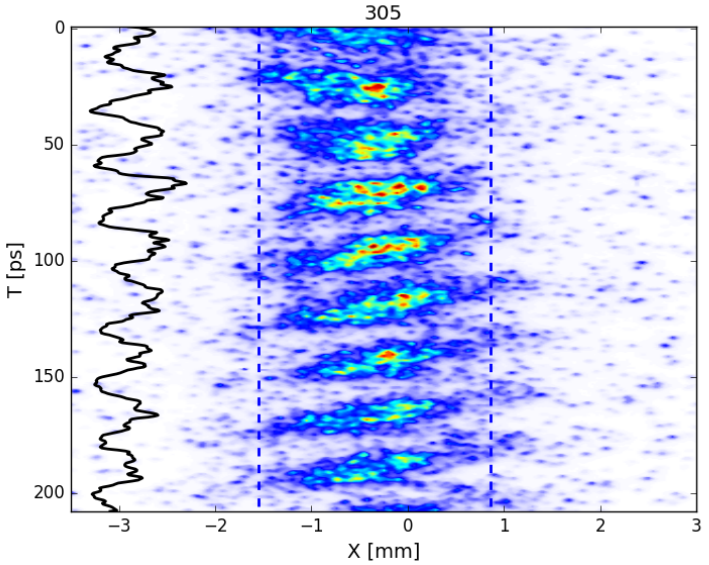

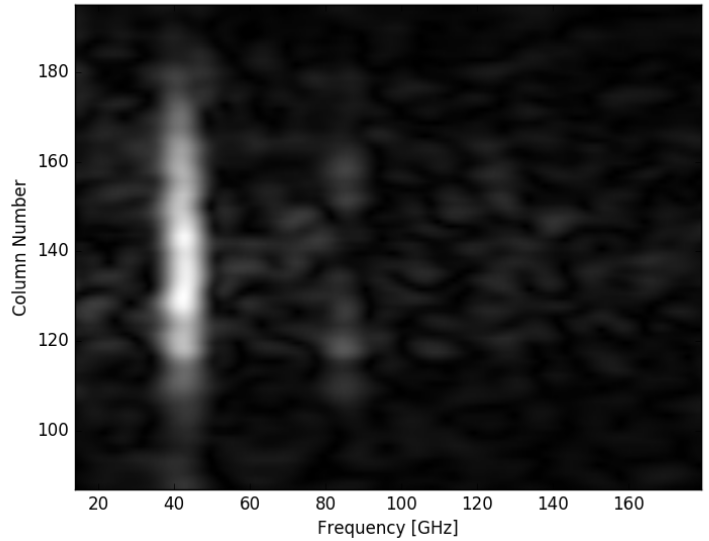

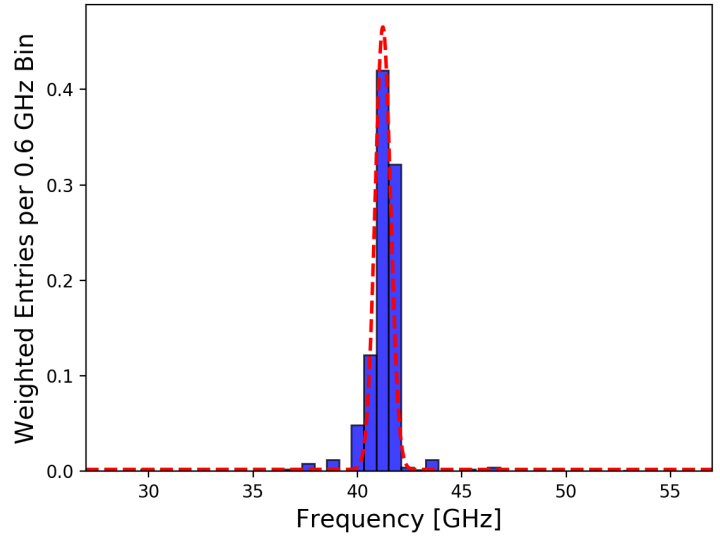

Streak Camera Optics (M. Martyanov)

M. Martyanov used a Ronchi Ruling to measure the point spread function (PSF) of the streak camera imaging system.

“Assuming the modulation depth of 0.12 we can mock up the Gaussian Green function, tuning its width such that to achieve given modulation depth of 0.12 from a square shaped signal. This procedure gives us the FWHM of Green’s function (the same as FWHM of point-like source) of 0.187mm - this is the estimation of optical resolution.”

8 pixels FWHM

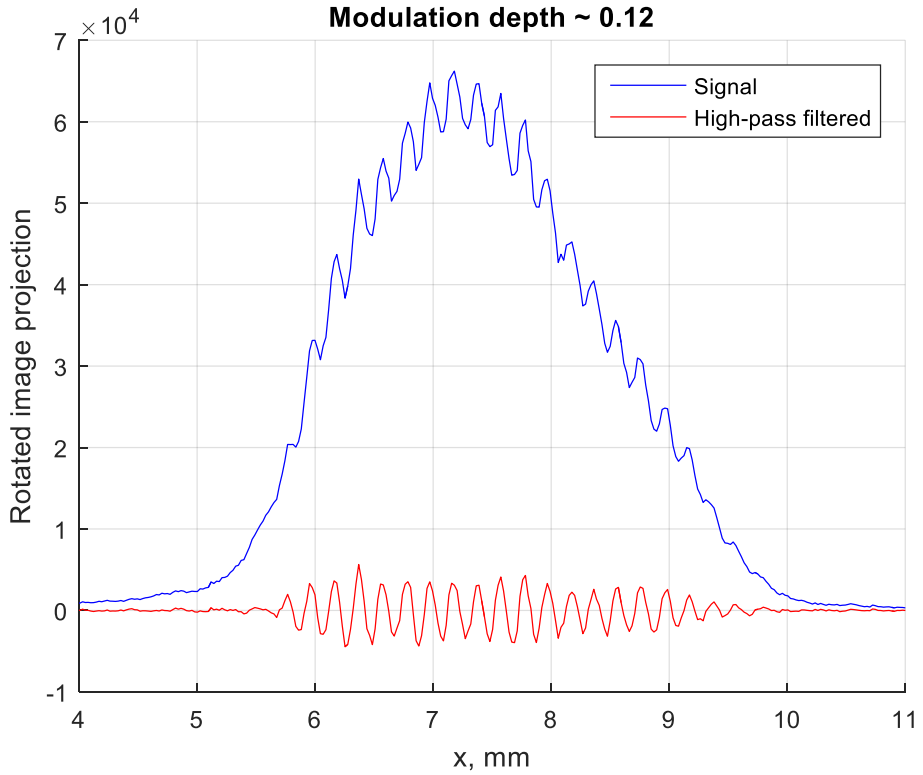

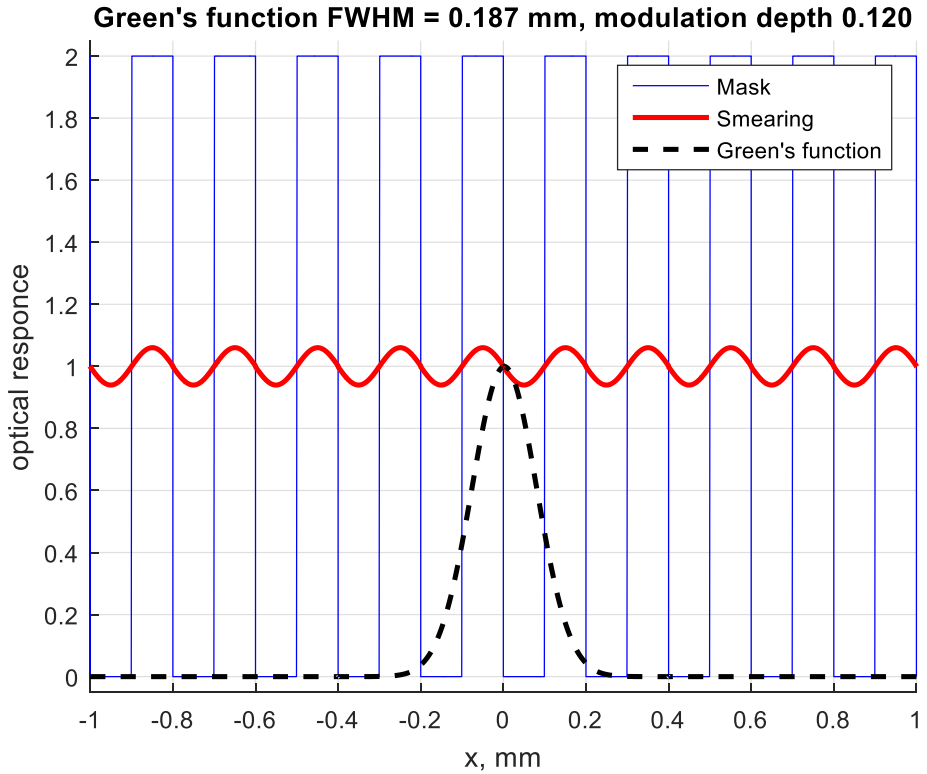

Covariance of the Data (A. Caldwell)

$$\mathrm{cov}_{ij} = \frac{1}{n_{evt} - 1} \sum_{n=1}^{n_{evt}} \frac{(f_i - \bar{f}_i)(f_j - \bar{f}_j)}{\sigma_{f_i} \sigma_{f_j}}$$

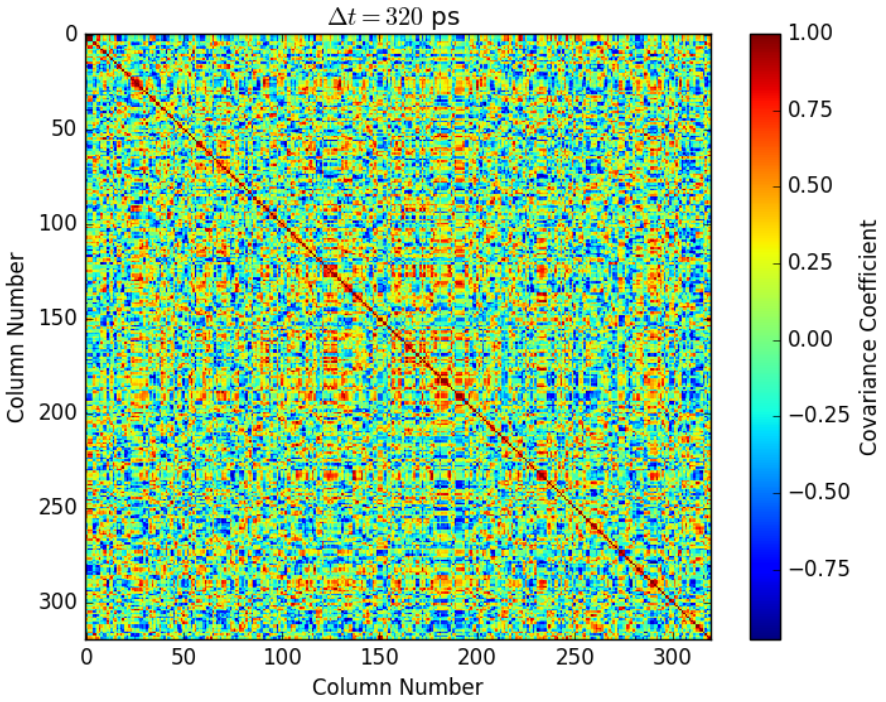

Computed for every column

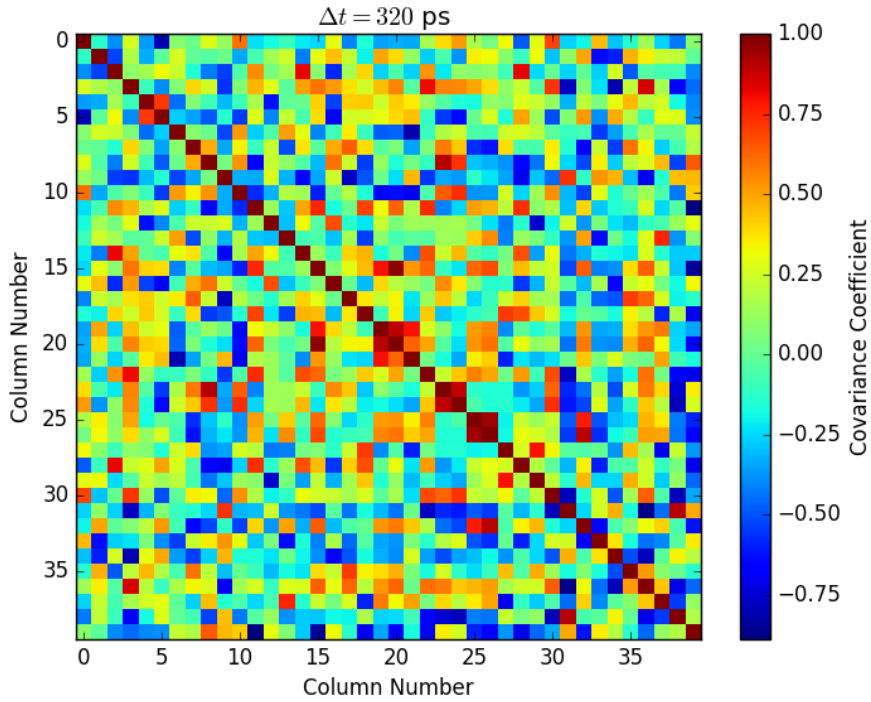

Columns binned in groups of 8 (optical resolution)

We calculate the covariance of the columns to check for correlations in the measurement. The central diagonal corresponds to the self-covariance (by definition = 1) whereas the off-diagonal measures covariance between different columns. If the covariance of the off-diagonal measurements is 0, then the measurements are independent.

Is each column an independent measurement?

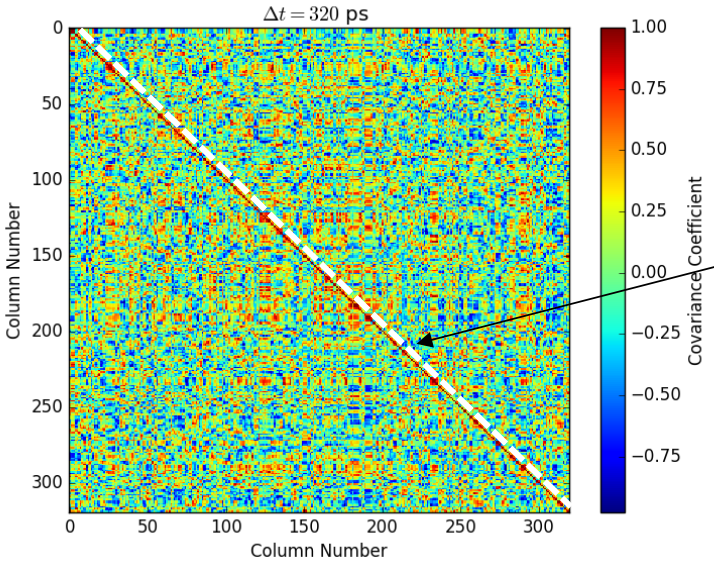

Computed for every column

Take the average of all elements 1 index off the diagonal, 2 index off the diagonal, 3 . . .

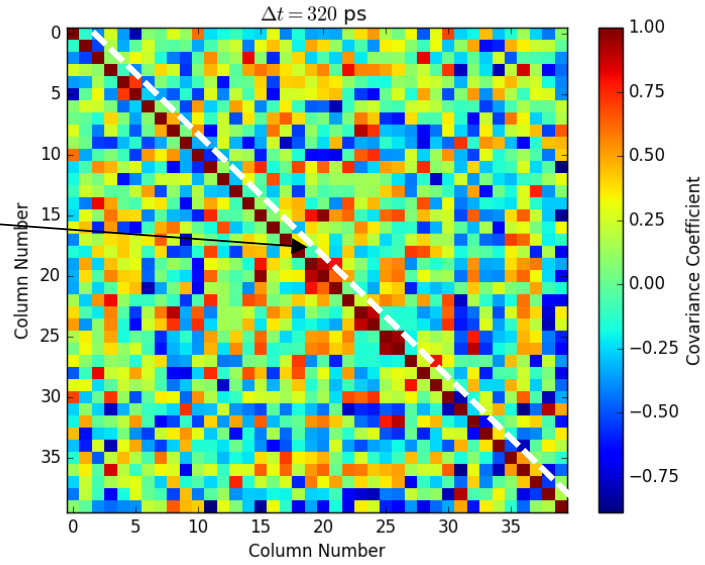

Columns binned in groups of 8 (optical resolution)

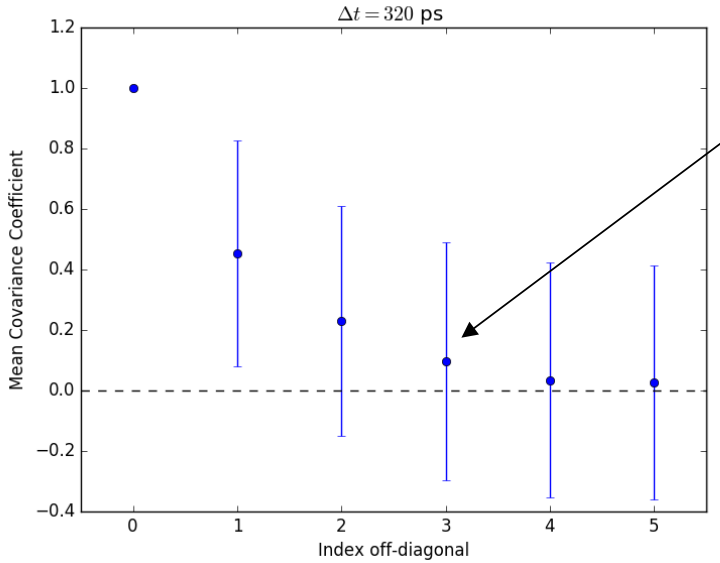

For every column case, correlation falls to zero after roughly 3 columns. This is consistent with 8 column FWHM (8/2.35 ≈ 3).

For 8 column binning, correlation immediately goes to zero.

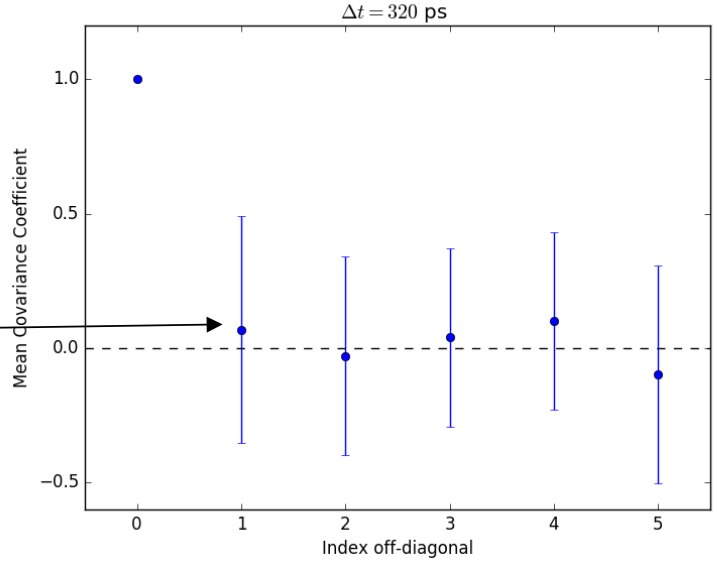

Binning columns by 8 produces independent measurements.

Results

For a given time delay and laser energy setting, all shots are added to a single histogram.

There are 40 binned columns per image, and shots per step, so each histogram has about 360 weighted entries.

The error on each bin is given by the sum of the bin weights squared. The fit function uses the errors and when performing the chi-squared minimization.

The error on the mean is extracted from the covariance matrix of the fit algorithm (SciPy curve_fit).

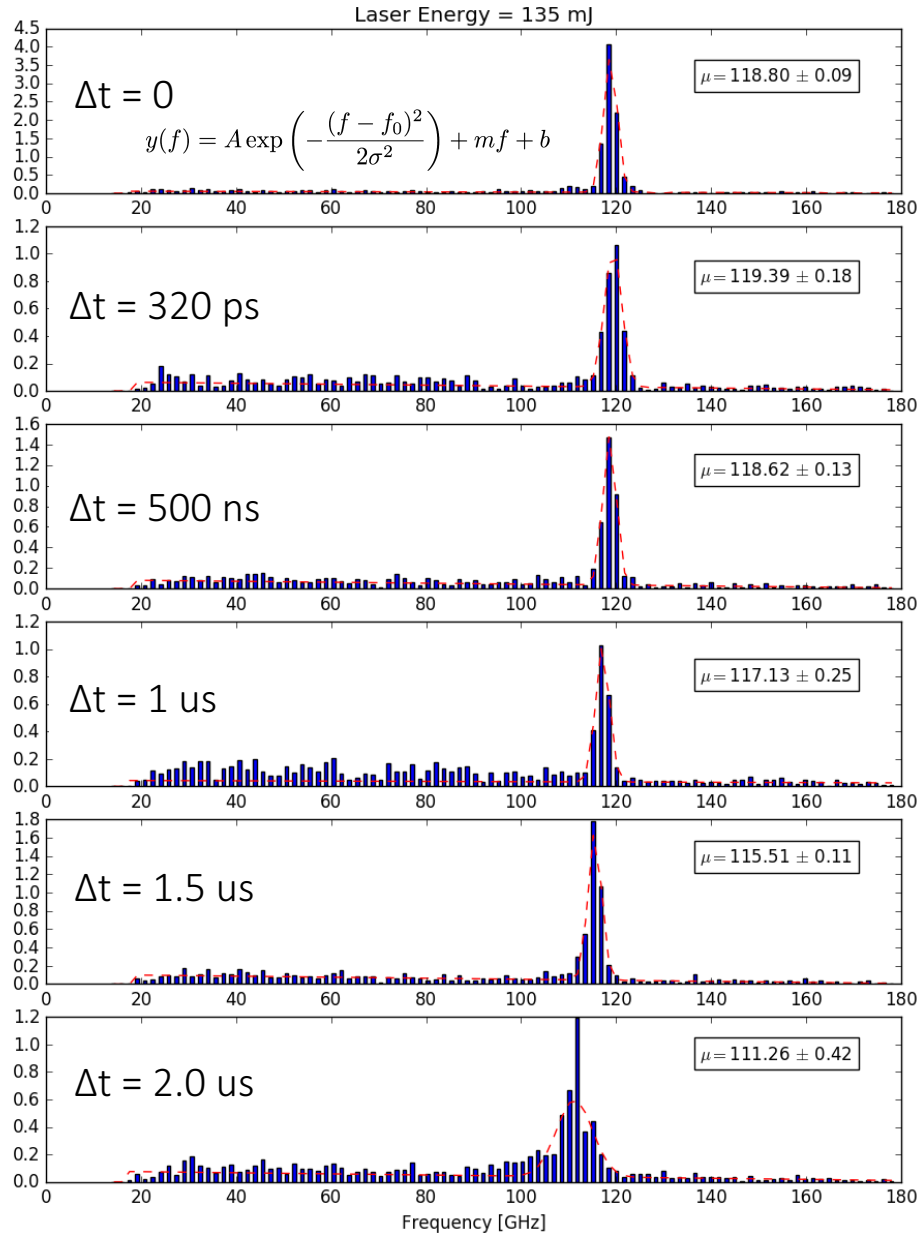

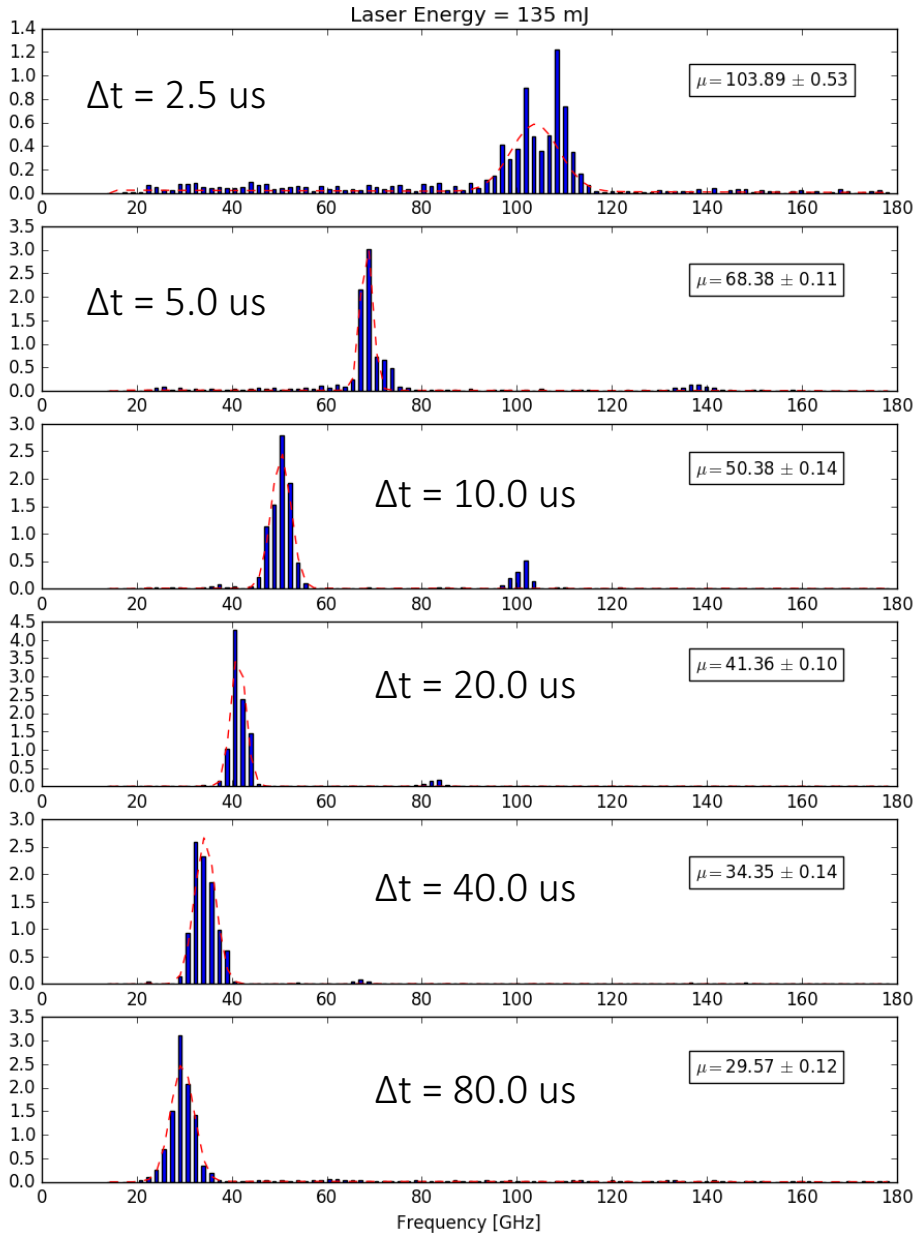

Uncertainty Values

Many people have noted that the uncertainties quoted in the paper appear to be small. For example, for time delay = 0, I cite an uncertainty of 0.09 GHz, which is much smaller than the resolution of the streak camera:

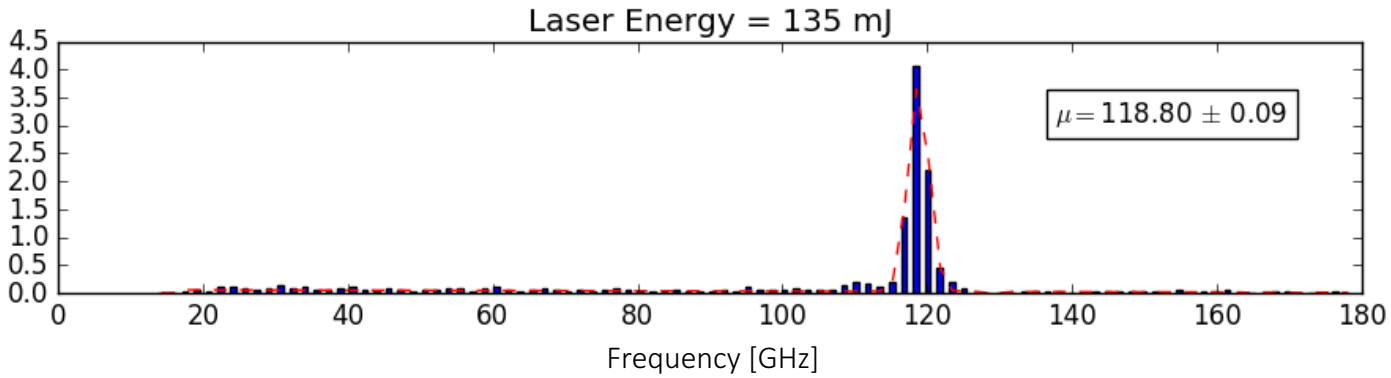

This is because I am citing the *error on the mean*. For gaussian distributed data with weight = 1, this is equal to:

$$\bar{\sigma} = \frac{\sigma}{\sqrt{N}}$$

where σ is the standard deviation of the data and N is the number of measurements

In the example to the left, the top distribution is much narrower than the bottom one, but it contains less measurements, and therefore has a similar uncertainty.

Examples

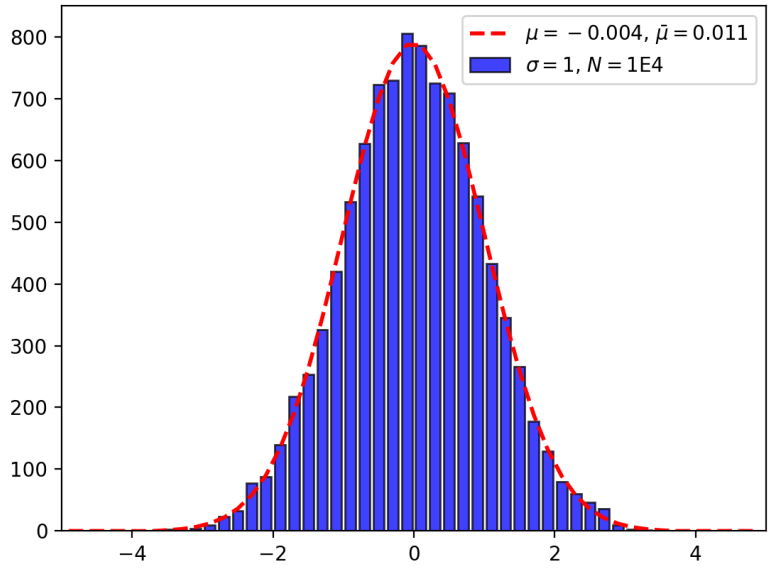

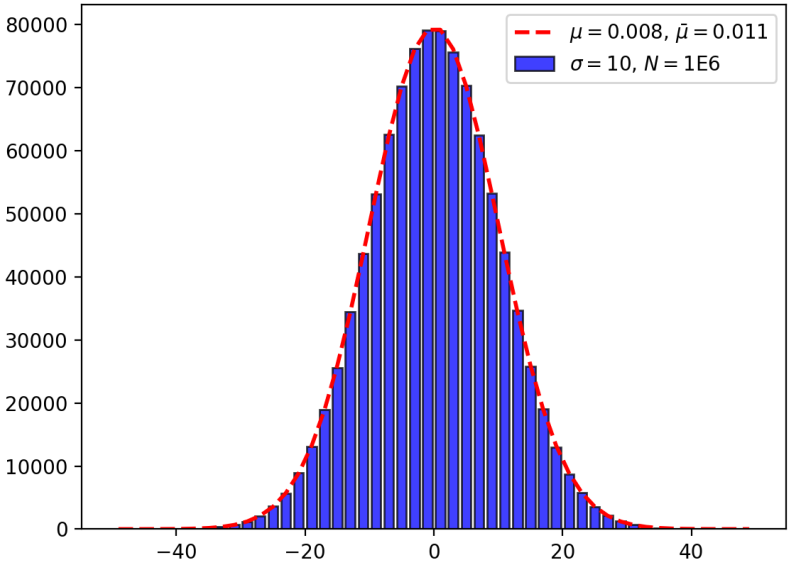

Outline

1. Measurement and Motivation
2. Data and Error Analysis
3. Model
4. Review of Figures
5. Updates to the Manuscript

Thermalization-Recombination Model

The original model came from Patric's work on the Lithium heat-pipe oven at FFTB (P. Muggli et al, "Photo-Ionized Lithium Source for Plasma Accelerator Applications", IEEE Plasma Science 1999).

The model describes the evolution of the plasma temperature and density. There is no spatial dependence. It boils down to solving a set of coupled ODEs:

$$\frac{dT_e}{dt} = \nu_{ei}(T_i - T_e) \qquad \frac{dn}{dt} = -\alpha_3 n^3$$

$$\nu_{ei} = 1.8 \times 10^{-19} \frac{(m_e m_i)^{1/2} n \lambda_{ei}}{(m_e T_i + m_i T_e)^{3/2}} \qquad \alpha_3 = 8.75 \times 10^{-27} T_e^{-4.5}$$

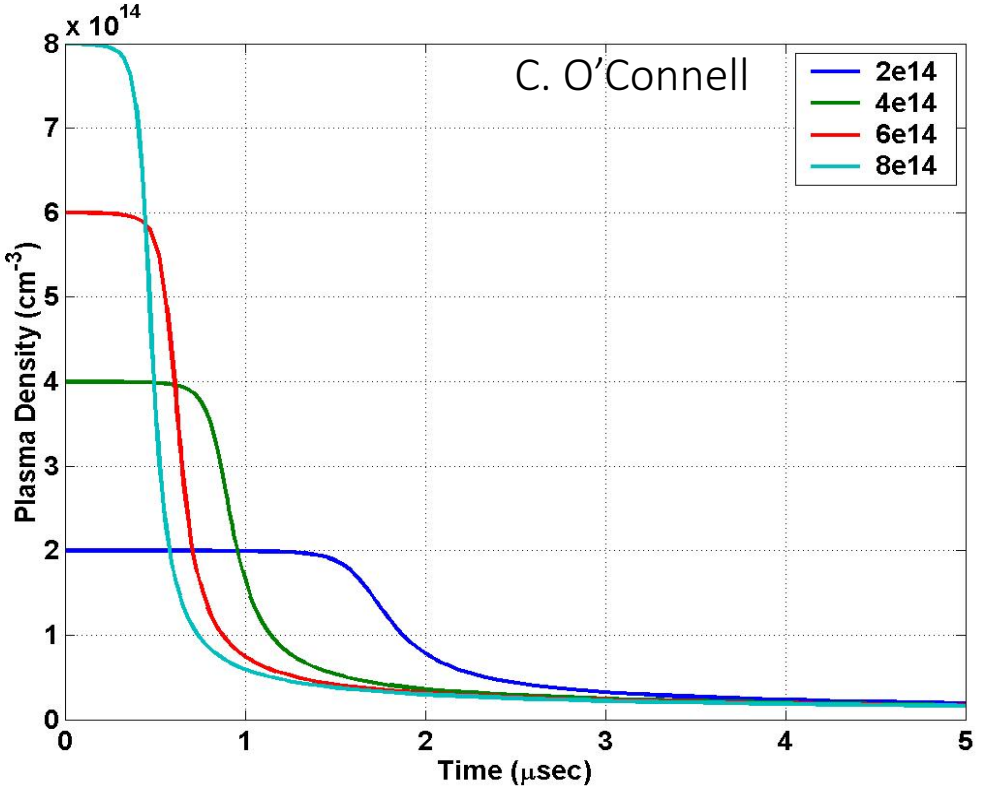

Konstantin pointed out that spatial effects might indeed be important. . .

Old Model

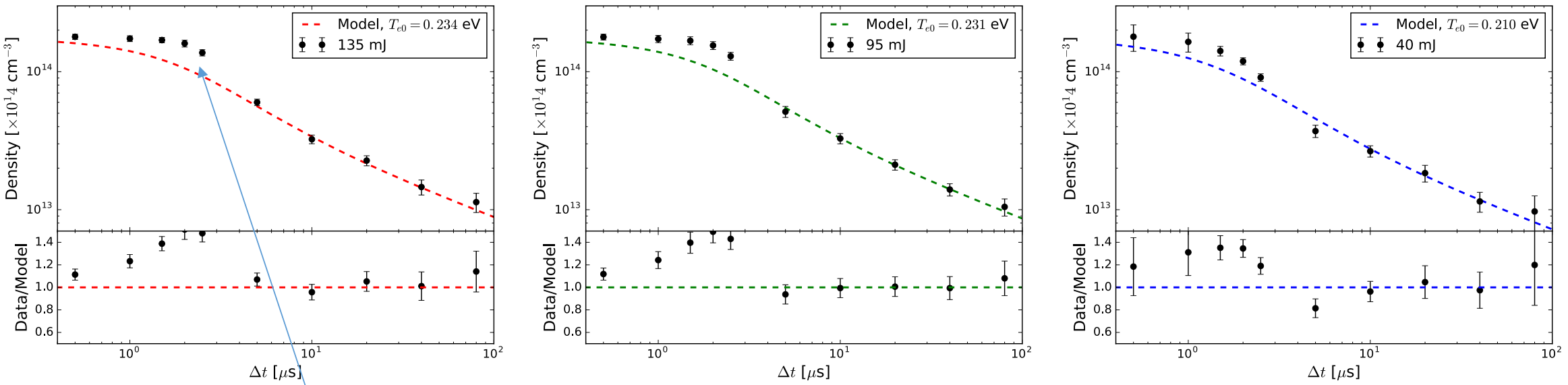

The ”uniform plasma” model does not predict the “knee” in the data.

New model includes spatial effects

Immediately after ionization, a plasma channel exists with radius r_0. The plasma electrons at the edge want to escape outwards. The ions don't let them move far. The electrons tug on the ions which diffuse into the neutral vapor. The rate of the diffusion is determined by the ion-neutral Rb cross-section. The ion-ion Rb cross-section is extremely large. Therefore, there is no diffusion at the center of the channel. The plasma in that region is trapped.

The result is an "etching" effect of the plasma column.

Modeling Ionization (G. Demeter)

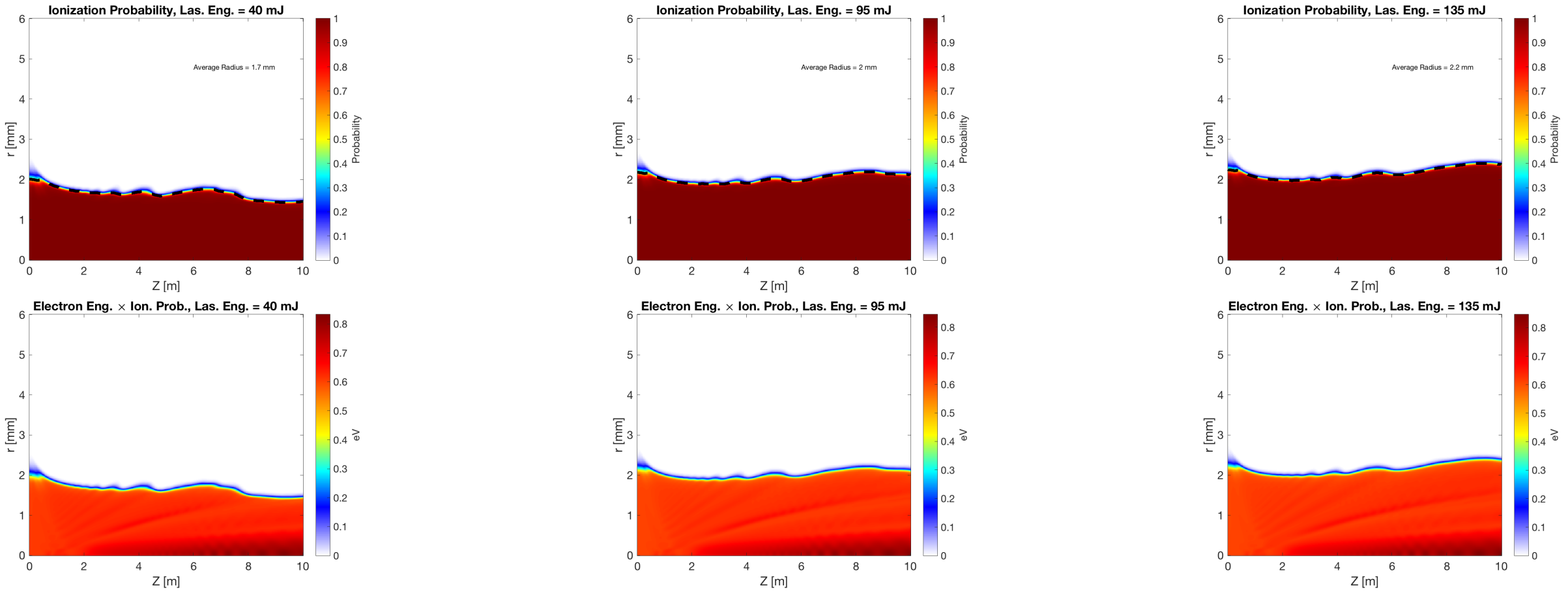

G. Demeter provided a model for laser ionization of rubidium ("Propagation of ultra-short, resonant, ionizing laser pulses in rubidium vapor". *PRA* 2019). We use the model as input for the initial ionized radius of the plasma column. The average ionized radius along the 10 meter cell is 1.7 mm for 40 mJ, 2.1 mm for 95 mJ, and 2.2 mm for 135 mJ. Note that the median plasma electron energy after ionization is 0.62 eV in all cases.

Plasma Fluid Model (V. Khudyakov and K. Lotov)

Vadim and Konstantin built a plasma fluid simulation to describe the evolution of the plasma column.

The simulation shows the “knee” that we see in the data. The knee occurs once the etching reaches the center of the plasma column.

However, the data and model do not agree exactly, and there were some computational challenges as well.

We abort trying to have a complete model of the plasma evolution.

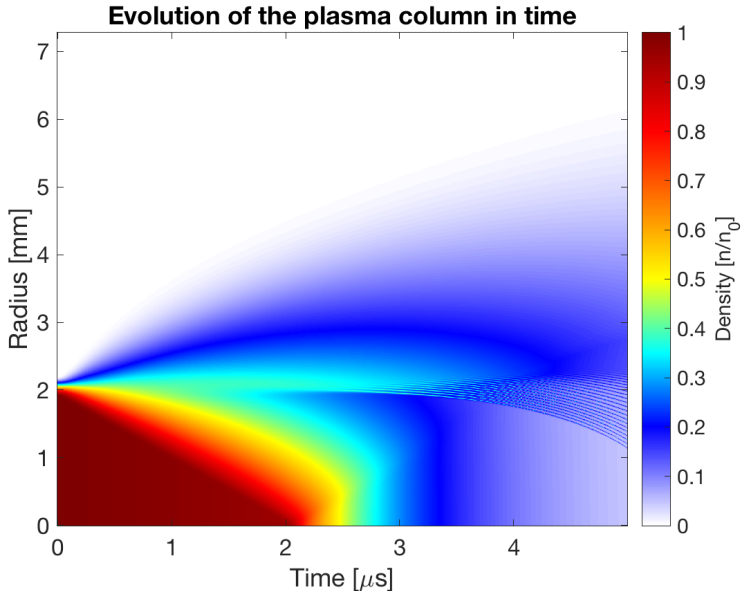

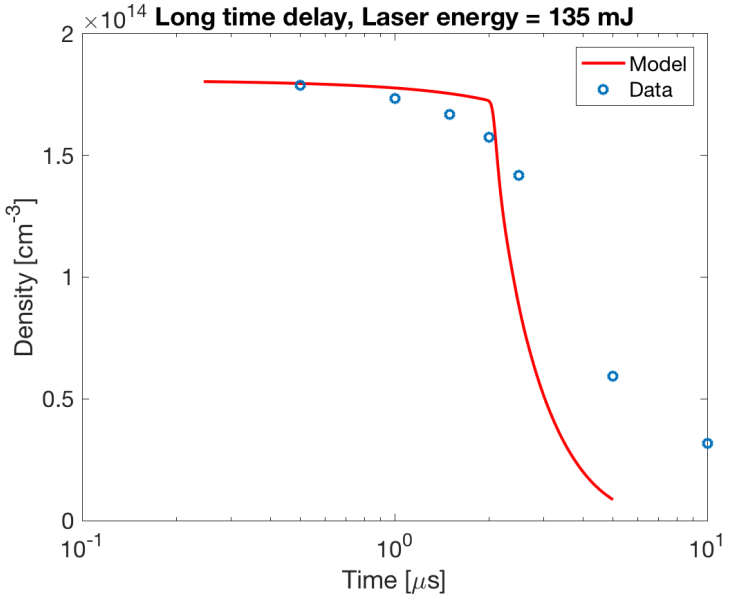

Fluid model

The plasma is characterised by density n, mean velocity $\mathbf{V}$ and electron and ion temperatures T_e, T_i. These quantities satisfy following equations.

1. Continuity equation with recombination
$$\frac{\partial n}{\partial t} + \nabla \cdot (n\mathbf{V}) = -\alpha_3 n^3.$$
2. Ion motion equation
$$m_i n \frac{d\mathbf{V}}{dt} = -\nabla p + \mathbf{R}_{fric},$$
where $p = n(T_e + T_i)$ – plasma pressure, $\mathbf{R}_{fric}$ – friction with neutrals.
3. Energy tranfer between electrons and ions
$$nT_e \frac{ds_e}{dt} = -\nabla \cdot \mathbf{q}_e + Q_{ei},$$
$$nT_i \frac{ds_i}{dt} = Q_{ie},$$
where $s_{e,i} = \ln(T_{e,i}^{3/2}/n)$ – density of entropy. Q – energy transfer between electrons and ions
$$Q_{ei} = -Q_{ie} = \frac{3m_e}{m_i}\frac{n}{\tau_e}(T_i - T_e)$$
$\mathbf{q}_e = -\kappa_e \nabla T_e$ – electron heat flow is also taken into account.
$$\kappa_e = 3.16\frac{nT_e\tau_e}{m_e},\ \tau_e = \frac{3\sqrt{m_e}T_e^{3/2}}{4\sqrt{2\pi}\Lambda e^4 n}$$

Friction with neutrals

Friction force originates from ion-neutral elastic collisions. Neutrals are considered motionless and collision cross-section is replaced by its mean value $\overline{\sigma} = \pi(2r_a)^2$, where $r_a = 0.25$ nm – radius of Rb-atom.

$$\mathbf{R}_{fric} = -mn_a n\langle\sigma(v)v\mathbf{v}\rangle = -mn_a n\overline{\sigma}\langle v\mathbf{v}\rangle = -mn_a n\overline{\sigma}V_T^2 \cdot \phi(V/V_T)\frac{\mathbf{V}}{V}$$

$m = m_i/2$ – reduced mass, n_a – density of neutrals, $V_T = \sqrt{T_i/m_i}$ – ion thermal velocity.

$$\phi \approx \begin{cases} \frac{8}{3}\sqrt{\frac{2}{\pi}}\frac{V}{V_T},\ V \lesssim V_T \\ \frac{V^2}{V_T^2} + 2,\ V_T \lesssim V \end{cases}$$

ϕ is calculated with Maxwell distribution $f(\mathbf{v}) = (2\pi V_T^2)^{-3/2}\exp(-(\mathbf{v}-\mathbf{V})^2/(2V_T^2))$.

Time-Dependent Ambipolar Waves

The “usual” diffusion equation is not sufficient to describe our experiment. This is because the diffusion constant changes rapidly from inside the plasma column to outside the plasma column.

The time-dependent ambipolar wave equation introduces a “free-expansion” term. Basically, the edge of the plasma column propagates outward like a wave.

For short times (less than the ambipolar collision frequency) we can neglect the diffusion term so this is just a wave equation.

THE PHYSICS OF FLUIDS VOLUME 8, NUMBER 9 SEPTEMBER 1965

Time-Dependent Ambipolar Diffusion Waves

Z. Shimony and J. H. Cahn
University of Illinois, Urbana, Illinois
(Received 14 December 1964; final manuscript received 19 April 1965)

A theory for the propagation of a plasma into an ambient gas is proposed. It is an extension of the usual ambipolar diffusion which takes into account the inertia of the particles and predicts a finite velocity for the propagation of the plasma. The equation

$$\nabla^2 n_e = (1/u^2)(\partial^2 n_e/\partial t^2) + (1/D_a)(\partial n_e/\partial t)$$

is obtained for the electron density in the expanding plasma, where $u = (D_a \nu_a)^{\frac{1}{2}}$, D_a is the ambipolar diffusion coefficient and ν_a is an “ambipolar collision frequency.” u gives the speed of propagation of the plasma interface and is equal to the velocity $(kT_e/M_i)^{\frac{1}{2}}$, if the electron temperature T_e is much higher than the ion temperature. This equation is solved in one-dimensional geometry and some characteristics of the solution discussed. It is shown that the maximum density of the plasma propagates with speed u in the case of low pressure of the gas but with much lower speed in the case of higher pressure.

JOURNAL OF APPLIED PHYSICS VOLUME 39, NUMBER 10 SEPTEMBER 1968

Free Expansion of an Isolated Plasma Column

Julius Hyman, Jr.*
University of California, Los Angeles, California 90024
(Received 5 January 1968; in final form 6 May 1968)

An isolated column of plasma is formed by the partial ionization of neutral argon gas with an intense, high-energy photon beam. The manner in which this plasma expands radially from its initial prescribed position is observed in a region where the plasma has no interaction with confining walls. It is shown that the expansion proceeds initially in accord with the wave equation, having a velocity of propagation $u \approx (\gamma k T_e/M_i)^{1/2}$, a value predicted theoretically by Shimony and Cahn. The driving force for the plasma expansion comes from the electrons, which are in turn cooled predominately by the adiabatic expansion.

Modeling Short Time Delay Behavior

For times $t < D_a/v_a^2$, we solve the 2D wave equation (assume uniform along z). We extract the on-axis plasma density at different times t and compare to the data.

Ambipolar Wave Equation

$$\frac{1}{v_a^2}\frac{\partial^2 n}{\partial t^2} + \frac{1}{D_a}\frac{\partial n}{\partial t} = \nabla^2 n$$

Ambipolar Velocity

$$v_a = (\gamma_r T_e/m_i)^{1/2} \approx \sqrt{D_a \nu_{i0}}$$

t = 0

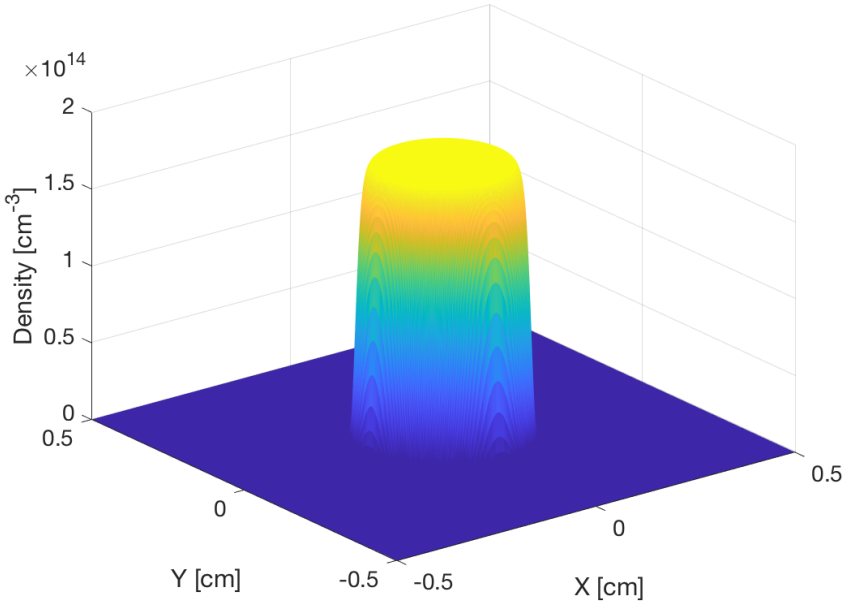

t = 1 μs

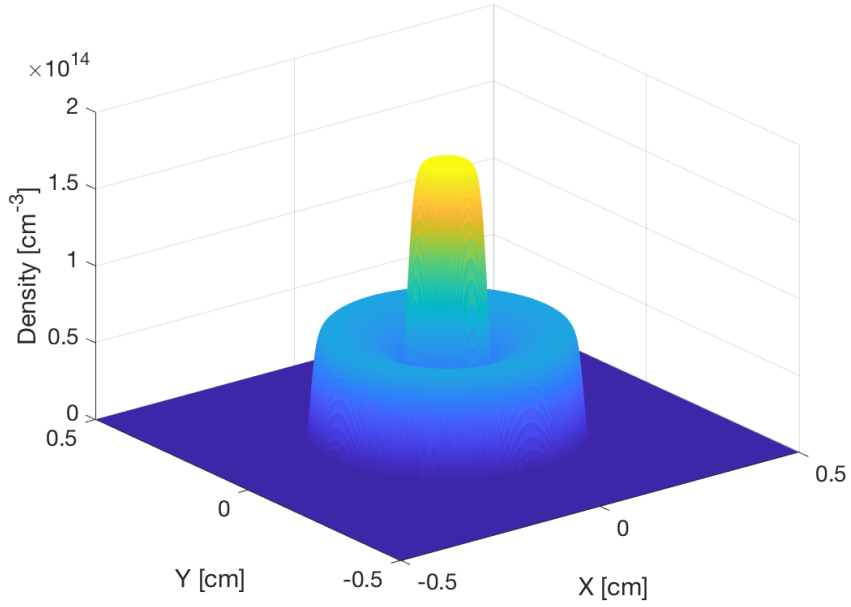

Comparing to Data

Best fit for 135 mJ data assuming T_{e0} = 0.41 eV

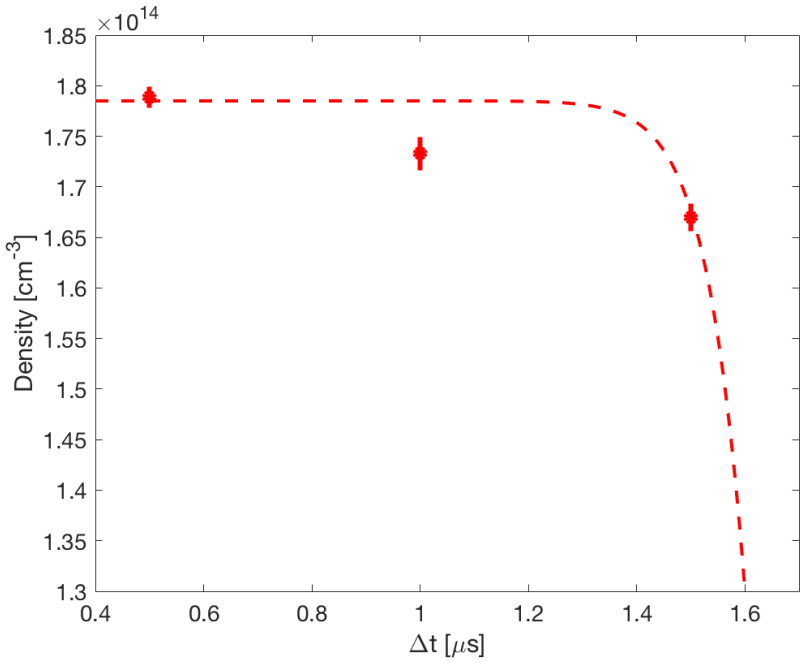

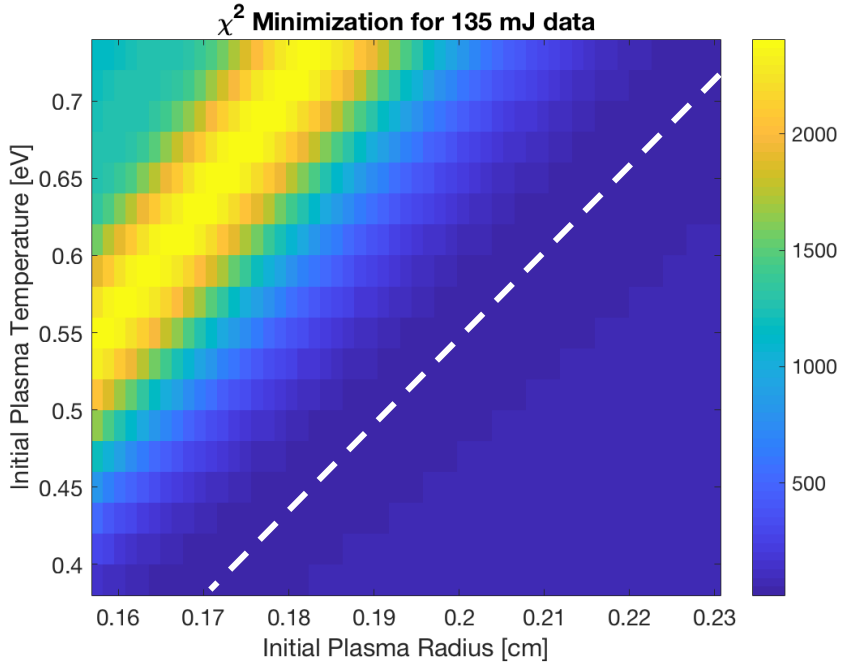

We use Gabor's model as an initial guess for the plasma column parameters, but we don't know the initial column width, or plasma electron temperature from the experiment. Therefore, we run the model for many combinations of the initial plasma radius and initial plasma temperature. Narrow, cold, plasma columns and wide, hot, plasma columns are both compatible with the data.

Comparing to Data

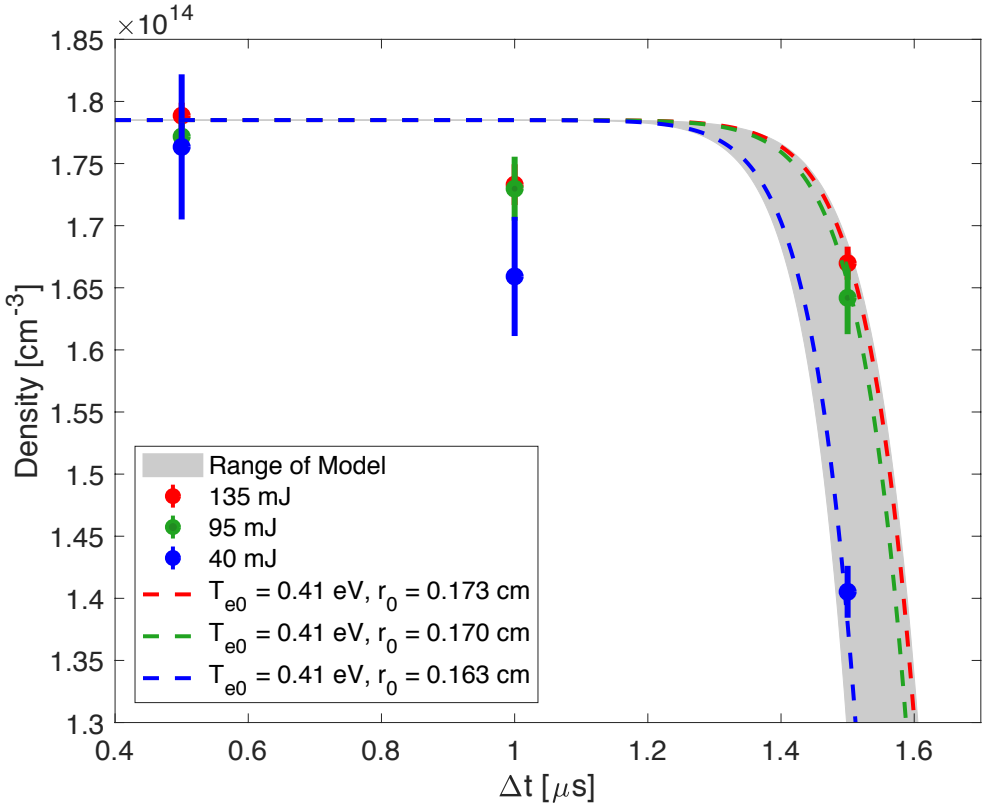

We say that the initial plasma temperature cannot be less than 0.39 eV (minimum ionization energy is 0.59 eV) or more than 0.73 eV (minimum ionization plus maximum of ponderomotive potential of the laser), which means that a range of plasma column radii are possible from 1.58 mm to 2.30 mm. The important thing is that the time it takes the ambipolar wave to etch away the plasma column is the same in all cases $t_{etch} = r_0/v_a$ = const.

Outline

1. Measurement and Motivation
2. Data and Error Analysis
3. Model
4. Review of Figures
5. Updates to the Manuscript

Figure 1

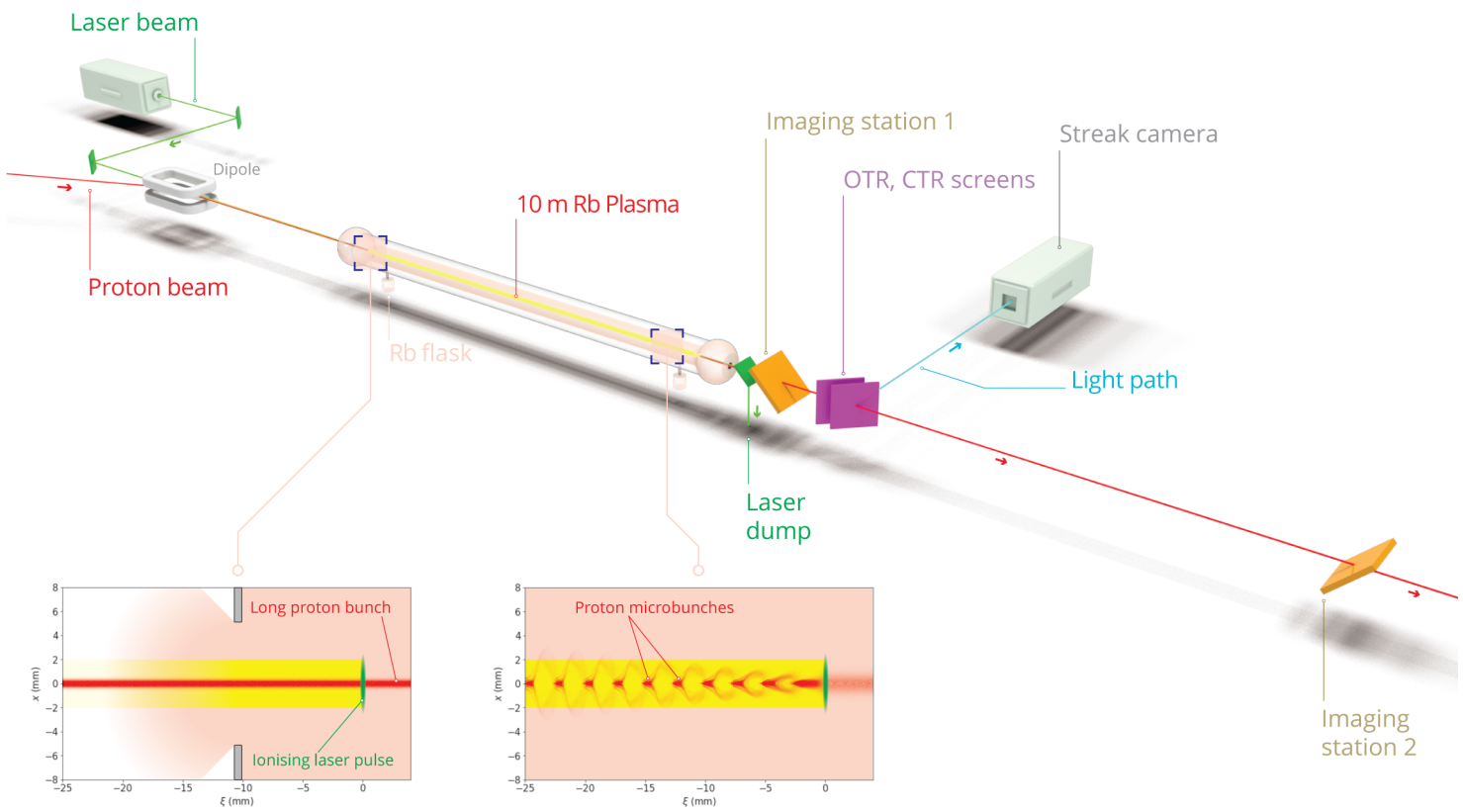

FIG. 1. Experimental layout of the AWAKE experiment showing key components. Dipole magnets and optical mirrors are used to align the proton and laser beams upstream of the vapor cell. Downstream of the cell, the proton beam passes through an OTR foil and optical light is generated in the process. The light is transported to a streak camera for temporal imaging. The inset illustrates a uniform, gaussian proton bunch entering the plasma which is micro-bunched by the time it exits the plasma.

Figure 2

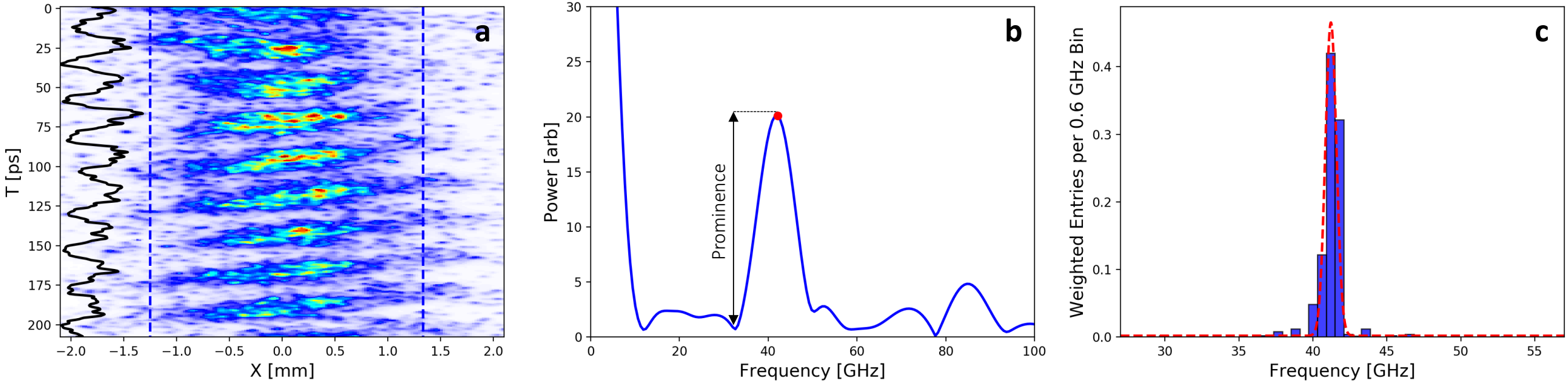

FIG. 2. a) Streak camera image of a modulated proton beam in a 200 ps-long time window. The vertical axis is the time axis, with $t = 0$ denoting the start of the window and not necessarily the start of the proton bunch. The horizontal axis is the transverse spatial coordinate with $x = 0$ located at the beam centroid. The ROI is denoted by dashed blue lines. The solid black line shows temporal projection of the image data in the region of interest. b) The absolute value of the FFT of the projection shown in a) after application of the analysis procedure described in Section III A. A peak in the spectrum is identified at 42.09 GHz using the peak-prominence algorithm and is denoted by the red circle. The prominence is denoted by the black arrow. c) Histogram of the peak frequencies identified with the column-by-column analysis technique. The entries to the histogram are weighted by their prominence and the histogram is fit with a gaussian centered at 41.57 ± 0.07 GHz, where the error on the centroid is extracted from the fit.

Figure 3

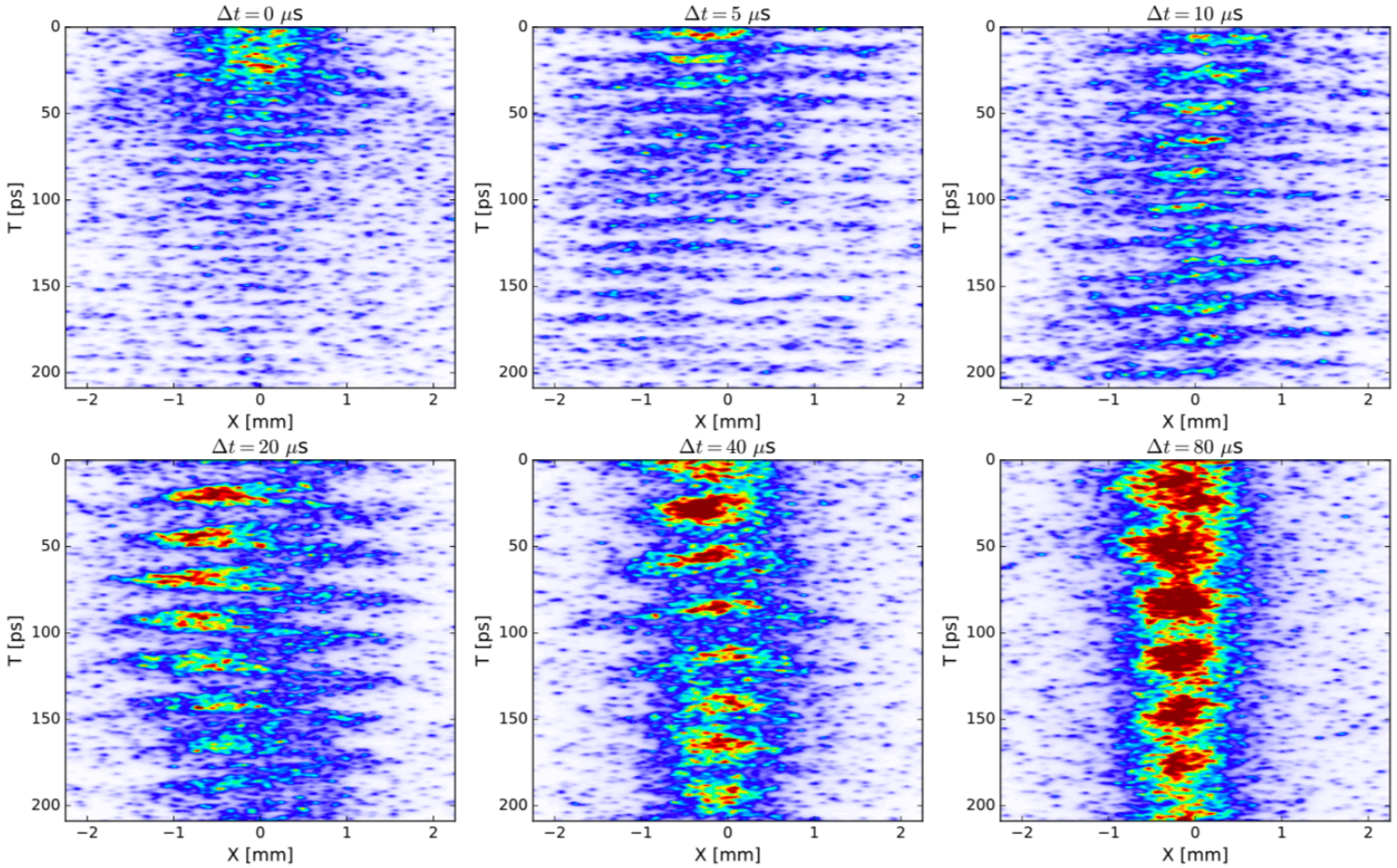

FIG. 3. Streak camera images of the modulated proton beam for example time delays Δt after ionization by the laser pulse with the high-power setting. The images share the same spatial, temporal, and color scales. The frequency of the modulation is clearly observed to be decreasing with time after ionization, indicating a decay in the plasma density. The image at a time delay of 20 μs has the signature of the hose instability which may arise in the case of un-seeded self-modulation.

Figure 4

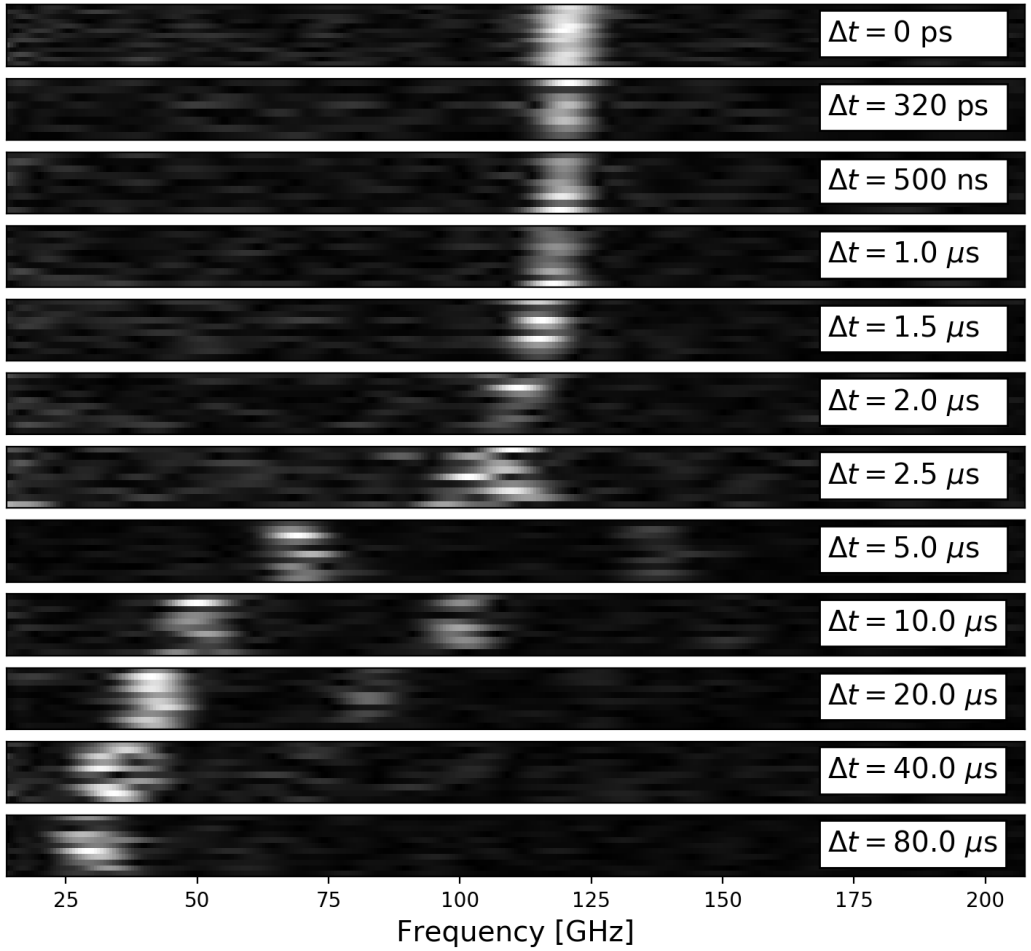

FIG. 4. Waterfall plot of the projected image data for the 135 mJ laser energy setting, with normalized color scale. Each subplot contains approximately 10 stacked Fourier spectra. The subplots are labeled by time after ionization, with 0 s at the top and 80 μs at the bottom. The larger time delays are logarithmically spaced. For time delays $\Delta t \geq 5$ μs, a second peak appears in the spectra at twice the frequency of the main peak. This may be due to the transverse hose instability, or harmonics in the main signal.

Figure 5

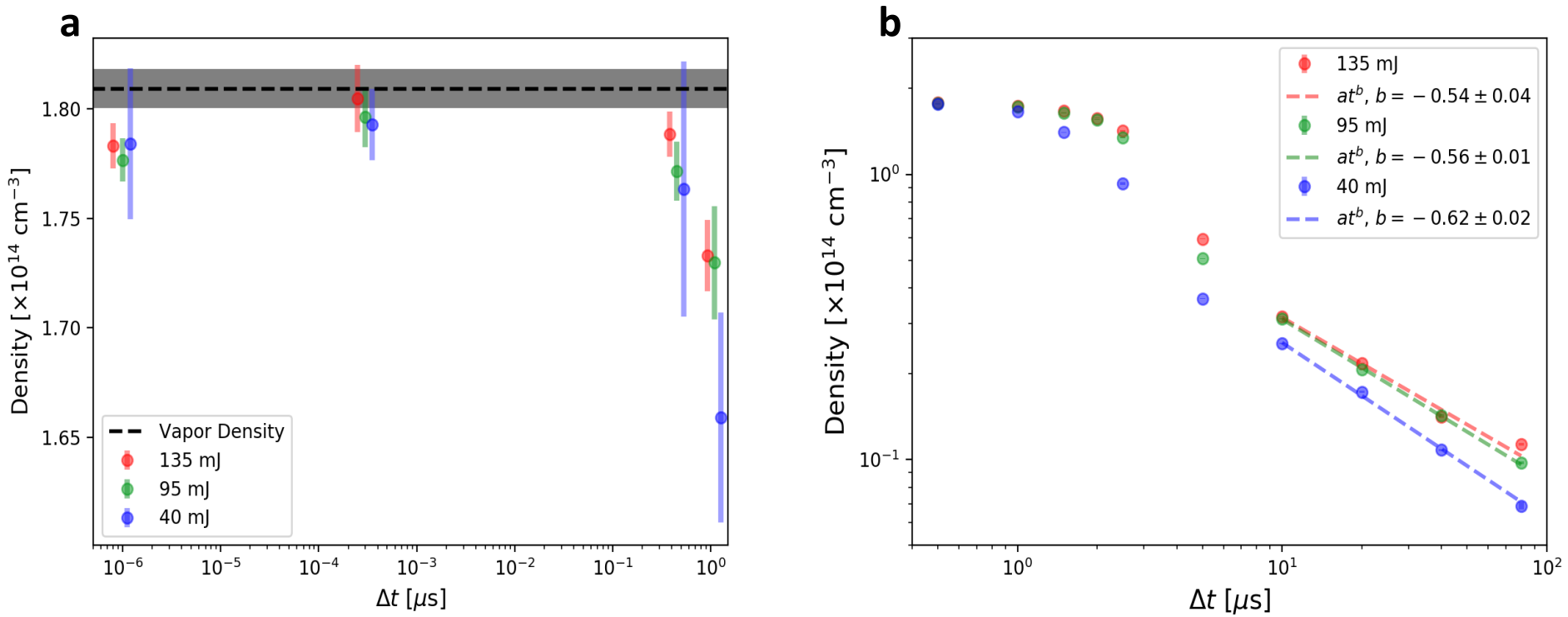

FIG. 5. a) Plasma density versus time after ionization for delays up to 1 μs, for the high, medium, and low energy laser settings, plotted on a log x-axis. The errors are shown multiplied by a factor of five so that they are visible in the plot. The measured vapor density with a 0.5% uncertainty is also shown. The data points corresponding to $\Delta t = 0$ s are assigned an offset of 1 ps so that they are visible in the plot. In addition, the high, medium, and low energy data points are assigned small temporal offsets so that the error bars are visible without overlap, but all groups of points are taken at the same time delay, namely 0, 320 ps, 500 ns, and 1 μs. b) Plasma density versus time after ionization for delays of 500 ns and greater. The data point corresponding to the low energy setting at $\Delta t = 2.0$ μs has been excluded due to noise in the signal. A power law fit of the form at^b is applied to the data for $\Delta t \geq 10$ μs.

Figure 6

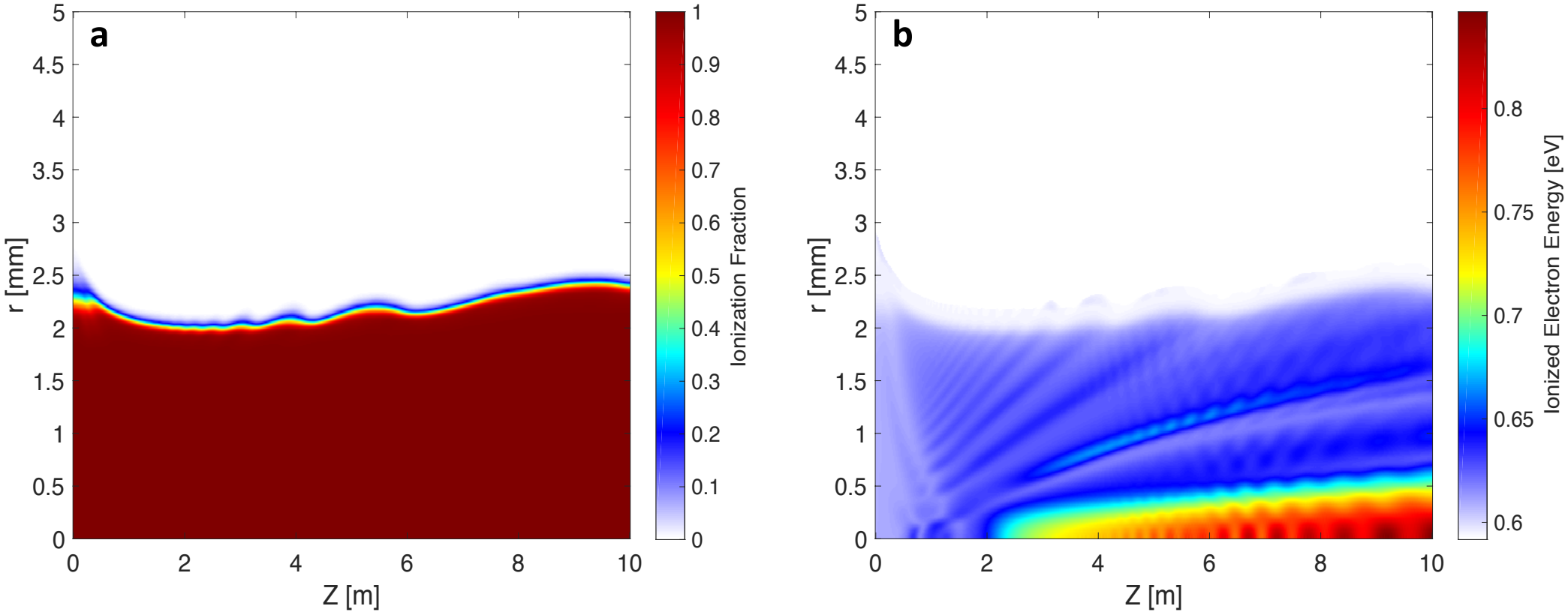

FIG. 6. a) Ionization fraction for the 135 mJ laser pulse setting with a gaussian transverse pulse shape based on the PPT model. The average radius of the ionized plasma column is 2.2 mm. b) Energy of ionized electrons. The minimum energy after ionization is 0.59 eV, while the median energy is 0.62 eV.

Figure 7

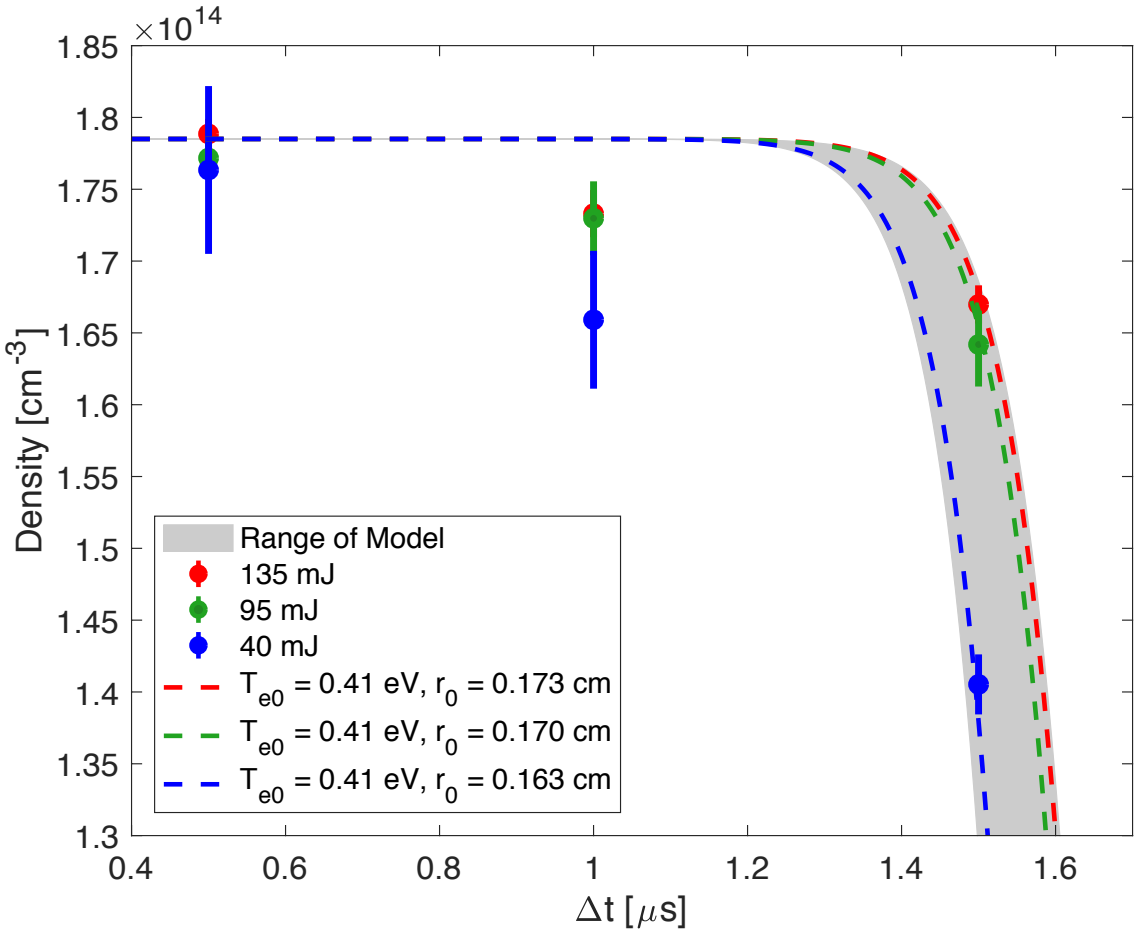

FIG. 7. Plasma density versus time compared to the on-axis density curves from the model. The red, blue and green data points correspond to the high, medium, and low energy laser settings, respectively, shown with error bars multiplied by five. The dashed lines are fits to the data at a fixed initial electron temperature of 0.41 eV. The shaded gray region shows the region of degeneracy of the model, where different values of T_e and r_0 produce similar on-axis density curves, so long as $t_{etch} = r_0/v_a \approx 1.5$ μs.

Outline

1. Measurement and Motivation
2. Data and Error Analysis
3. Model
4. Review of Figures
5. Updates to the Manuscript

Updates to Manuscript

Aside from the many typos and small comments, here are the substantive changes to the manuscript from the version sent last week:

1. Updating the language and numbers when discussing laser spot size and Rayleigh length
2. Including the resolution when discussing projection vs. column-by-column analyses
3. More details regarding covariance, weighting, statistics, etc in Section 3.B “Statistical Approach”
4. Explicit mention of the laser propagation model in Section 5.A “Plasma Formation”
5. Adding discussion of finite beam size when describing Figure 7.
6. Clarifying language in modeling section.
7. Rewriting of the conclusion regarding plasma relaxation time.

Which journal?

Physical Review X

Physical Review X (PRX) is an online-only, fully open access journal that places a high value on innovation, quality, and long-term impact in the science it publishes. It seeks to publish a select set of papers from all areas of pure, applied, and interdisciplinary physics that have the potential to influence current and future research and to have a long-lasting and profound impact in their relevant fields.

Breaking New Ground in Physics

Reflecting the diversity and dynamics of today's physics research, PRX showcases research in established core areas of physics that achieves breakthroughs in technology, experiment, and theory, or that represents a paradigm shift in understanding. The journal also publishes creative, impactful research that brings together multiple physics fields, or bridges physics with other disciplines.

PRX is very selective at the editorial level. If rejected by the editors, we can go for Physics of Plasmas.